12-25-2008

Structure and Dynamics of Metalloproteins in Live Cells

Jeremy D. Cook
Wayne State University

James E. Penner-Hahn
University of Michigan

Timothy L. Stemmler
Wayne State University, tstemmle@med.wayne.edu

This is the author's post-print version, previously appearing in Methods in *Cell Biology*. 2008, v. 90 p. 199-216.
Available online at: http://www.elsevier.com/

Structure and Dynamics of Metalloproteins in Live Cells

Jeremy D. Cook[1], James E. Penner-Hahn[2,*] and Timothy L. Stemmler[1,*]

[1]Department of Biochemistry and Molecular Biology, Wayne State University, School of Medicine, Detroit, MI

[2]Department of Chemistry, The University of Michigan, Ann Arbor, MI

[*]Corresponding Authors: James E. Penner-Hahn, Department of Chemistry, The University of Michigan, 930 N. University, Ann Arbor, MI 48109, Ph: (734) 764-7324, jeph@umich.edu; Timothy L. Stemmler, Department of Biochemistry and Molecular Biology, Wayne State University, School of Medicine, 540 E. Canfield Ave, Detroit, MI 48201, Ph: (313) 577-5712, tstemmle@med.wayne.edu.

Abstract

X-ray absorption spectroscopy (XAS) has emerged as one of the premier tools for investigating the structure and dynamic properties of metals in cells and in metal containing biomolecules. Utilizing the high flux and broad energy range of X-rays supplied by synchrotron light sources, one can selectively excite core electronic transitions in each metal. Spectroscopic signals from these electronic transitions can be used to dissect the chemical architecture of metals in cells, in cellular components and in biomolecules at varying degrees of structural resolution. With the development of ever-brighter X-ray sources, X-ray methods have grown into applications that can be utilized to provide both a cellular image of relative distribution of metals throughout the cell as well as a high-resolution picture of the structure of the metal. As these techniques continue to grow in their capabilities and ease of use, so to does the demand for their application by chemists and biochemists interested in studying the structure and dynamics of metals in cells, in cellular organelles and in metalloproteins

Introduction

Metalloproteins, proteins that bind metal cofactors, make up a substantial portion of the human proteome and are essential for the viability both of individual cells and of the overall organism. By some estimates, as many as one-third to one-half of all proteins are metalloproteins (Ascone et al., 2003). Both the reactivity and indeed even the structure of a protein can change when a metal binds to the organic protein peptide chain. These changes often allow the resulting metalloprotein to accomplish unique chemistry and maintain unique folds that could not be accomplished in the absence of metal. For example, the oxygen binding ability of hemoglobin and the CO_2 hydration activity of carbonic anhydrase have an absolute dependence on the presence of, respectively, heme iron and a divalent cation (typically zinc). Given the versatility in chemistry that each metal can perform, it is no surprise that metalloproteins are selective in the metal they accept, and different metals are utilized to a greater degree in different regions of the cell and in the organism. However, the chemical reactivity provided by metals can be both a blessing and a curse, especially when cellular pathways for metal homeostasis fail. Friedreich's ataxia and Wilson's disease are just two examples of hereditary disorders that are linked to failures in metal homeostasis: iron in the case of Friedreich's ataxia and copper in the case of Wilson's disease. In both diseases, a breakdown in a single component of the complex cellular metal-processing machinery has highly deleterious consequences to the organism.

Cells have therefore developed complex and comprehensive protein controlled mechanisms to ensure that metal homeostasis proceeds in an unhindered fashion. At the molecular level, placement of a specific metal, and only the appropriate metal, in the correct protein binding site is essential. At the same time, the protein based ligand environment surrounding the metal helps to control the chemical reactivity of the metal (e.g., the porphyrin ring and hydrophobic ligand binding pocket in hemoglobin help promote reversible O_2 binding and release in favor or CO binding and/or formation of μ-oxo bridged hemes, two reactions that are favored in solution). The individual components of the cellular homeostasis machinery include metal specific pumps to bring the metal into the cell or cellular organelle, metal chaperones that selectively deliver metal to the metalloprotein partner and transcriptional regulation proteins that control the process at the genetic level. To fully understand and appreciate this machinery, it is necessary to understand both the details of the individual protein components, especially at the metal center, and the ways in which these parts interact to form the whole.

RATIONALE

Although genetics studies have proven to be highly effective in helping determine the global role of metalloproteins within the complex machinery of cellular metal homeostasis, a complete understanding of how this cellular machinery functions requires knowledge of how the individual components operate. For metals, functional characterization begins with a thorough understanding of the metals themselves, over a range of distance scales from cellular to atomic. At the cellular level, studies of the distribution of each metal within the cell provide a general blueprint of cellular metal homeostasis. Characterization of metal site/structure at the cellular organelle level allows one to focus on how metals are compartmentalized and generally utilized within unique regions of the cell. Finally, characterization of metals at the atomic level provides a high-resolution picture of how metalloproteins utilize each metal. While no single technique can answer all of these questions, modern X-ray methods have provided valuable insights at all of these dimensional scales. The goal of this report is to describe two X-ray based techniques currently employed to characterize metals in cells at different degrees of resolution: X-ray absorption spectroscopy and X-ray fluorescence imaging.

The extremely high flux of tunable X-rays available at synchrotron radiation laboratories has dramatically expanded the range of applications that can be utilized to characterize metals in cells at different degrees of resolution. X-ray Absorption Spectroscopy (XAS) is an element-specific probe of the local structural environment of a metal (Scott, 1985). XAS includes both extended X-ray absorption fine structure (EXAFS), which gives information on the bond-lengths, and X-ray absorption near-edge structure (XANES), which gives information on metal geometry and oxidation state. By making measurements on intact whole-cells, these properties can be exploited to characterize the *average* structural environment for each of the metals in a cell. In those cases where average information is not sufficient, it is necessary to enhance the resolution, either by imaging or by purification. X-ray fluorescence (XRF) imaging can provide nm scale detail regarding the distribution of metals within cells, but only rarely provides the spectroscopic detail available from XAS. Alternatively, XAS can be used to provide high-resolution details for purified metalloproteins. This provides the highest accuracy structural information, but with the loss of detail regarding spatial distribution within a cell. In the following, we provide a general description of each technique, outline what is required to collect and analyze each type of data and finally provide specific examples of how each technique has been employed to directly address questions regarding metals that are predominately bound to proteins within cells.

METHODS

X-ray Absorption Spectroscopy

XAS can be utilized to determine the high resolution electronic and structural details of metals bound to a single protein sample under a variety of different conditions (substrate vs. inhibitor bound, different metal oxidation states, etc.) or for each metal-bound molecule in a multiprotein complex. Sample constraints for the technique require metal concentrations of at least 0.1 - 0.3 mM (although higher is better) and solution volumes generally between 50 and 150 μL. Solution samples must be frozen quickly, typically with glassing agents present, in order to avoid ice formation and the absorbing element's atomic number in most cases must be bigger than ~19 (i.e., first transition series elements or heavier), although some very nice work has been done on lighter elements, such as sulfur. Questions typically addressed using this technique include: 1) what is the average oxidation state of the metal(s) in the sample, 2) is the metal site affected by the presence of substrates, inhibitors, redox agents, etc., 3) what is the ligand environment around the metal and 4) is the metal part of a multinuclear cluster in the protein under investigation?

The XAS method utilizes intense monochromatic X-rays from a synchrotron light source to excite the core electrons in the absorbing atom (A) of interest. When the electron is excited to the continuum, the resulting photoelectron wave is scattered by the neighboring atoms (S, the scattering atom). For iron, the electron excitation edge occurs at ca. 7130 eV, as shown in the XANES region of Figure 1. Information regarding the average oxidation state, ligand coordination geometry, and symmetry of the absorbing atom can be obtained from analysis of the XANES region of the XAS spectrum. In Figure 1, the EXAFS refers to the modulations in the absorption coefficient on the high energy side of the absorption edge. EXAFS oscillations occur as a consequence of the fact that, depending on the wavelength of the photoelectron wave, the outgoing and backscattering waves can overlap either constructively or destructively to give maxima (E_1) and minima (E_2), respectively, in the absorption coefficient. Simulations of the EXAFS region can be used to determine the average metal-ligand bond distances with good resolution (~0.1 Å), very good accuracy (~ 0.02 Å) and outstanding precision (~0.004 Å). Metal-ligand coordination numbers can be determined to ± 1 and ligand type can be determined to within a row of the periodic table (i.e., oxygen can be distinguished from sulfur, but not from nitrogen atoms). The information from XAS is thus similar to that obtained from protein crystallography, but without the need for diffraction quality crystals. The overall information content of protein crystallography is much higher, but even when a crystal structure is available, it is often the case that XAS can nevertheless provide unique information regarding the metal site structure (Tobin et al., 2003).

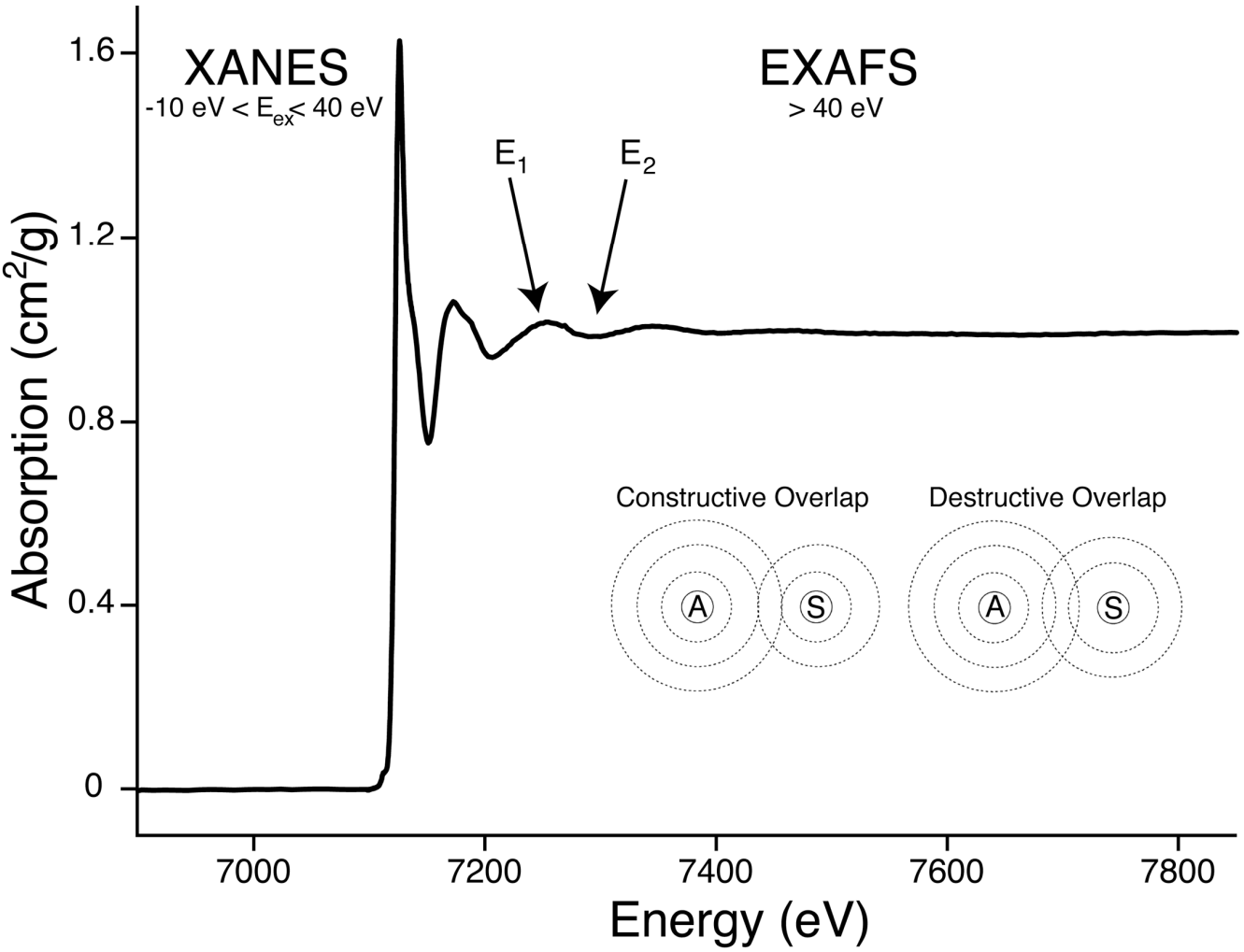

Figure 1: Iron K-edge XAS spectrum from ferrous ammonium sulphate. Spectra are divided into the XANES region (- 10 eV to + 40 eV relative to the large excitation signal) and the EXAFS region (> 40 eV above the excitation edge). In the EXAFS region, absorption maxima (E_1) and minima (E_2) are highlighted. Inset: constructive and destructive overlap of photoelectron wave generated from excitation of the iron 1s core electron to the continuum.

Purified Protein XAS

Historically, almost all biological XAS studies have been performed on purified proteins. This is because XAS is a "bulk" spectroscopy, (i.e., it is sensitive to all of the forms of an element that are present in a sample). If the element of interest is present in two different forms, the resulting XAS spectrum will be the weighted average of these two. Thus, a protein that contains one $ZnCys_2His_2$ site and one $ZnCys_4$ site would be indistinguishable from a protein containing two $ZnCys_3His$ sites. A particularly problematic case is protein samples that are heterogeneous, for example with a mixture of active site metal and adventitious metal.

Whole Cell XAS

Despite the limitations inherent in averaging, there has been growing use of XAS to characterize the *average* coordination structure and electronic properties of heterogeneous samples. Whole cell XAS can be utilized as a direct method for determining the average metal chemistry within the entire cell. The element specificity of X-ray absorption allows one to answer specific questions regarding the form of *each* metal in the cell. Virtually any form of sample can be used, with examples including whole blood in tunicates, intact biological tissue, isolated bacterial cultures or even soil samples. Measurements are made in the same way as conventional X-ray absorption. Because the resulting data represents a weighted average of all of the chemical environments of the element of interest, it can be difficult to use with complex mixtures, although there has been some success in modeling the resulting spectra as linear combinations of reference spectra. This is particularly true for elements such as sulfur (Gnida et al., 2007; Pickering et al., 1998), where there is dramatic spectral variation for different chemical species. One common application of whole-cell XAS is for samples where an exogenous metal (perhaps a toxin or a drug) has been added to the sample. In such cases, the absence of an endogenous form of the metal can simplify analysis since the element of interest may be present in only one predominant form. In this case, whole cell XAS can be used to determine the chemical state of the added metal, for example, the form in which metals are stored in a metal tolerant organism.

X-ray Fluorescence Imaging

With modern, so-called "third generation" synchrotron sources, it is possible to focus high-flux, high-energy X-ray beams to very small spot sizes (~150 nm or smaller). This beam can be rastered across a sample in order to obtain spatially resolved data (Paunesku et al., 2006b). The simplest experiment is to record the intensity of X-rays emitted from each point in the sample. Since each element emits X-ray fluorescence at a characteristic energy, the resulting emission spectrum permits direct determination of the composition of a sample. By recording XRF spectra at each point in a sample, it is possible to construct a map of the spatial localization of each element heavier than phosphorus (lighter elements can, in principle, also be imaged, however this generally requires that samples be mounted in a vacuum chamber). With proper calibration, XRF images can provide absolute elemental concentrations. Most XRF imaging has been performed on thin samples, but it is also possible to extend the technique to three dimensions, using tomographic reconstructions to obtain the complete three-dimensional distribution of an element.

Combined Spectral and Spatial Resolution

X-ray fluorescence is essentially an atomic phenomenon – that is, the XRF signal is virtually independent of the chemical environment of the atom. Thus, an iron XRF map provides information on the local Fe concentration, but no insight as to whether this is due to a heme protein, a Fe/S protein or the iron-oxide core of ferritin. To get around this limitation, it is possible to combine XRF imaging with XAS spectroscopy using either microXAS or XANES imaging (Pickering et al., 2000). If one measures the complete XAS spectrum for a spatially resolved portion of the sample (so-called microXAS), it is possible to determine the chemical form (or at least the average chemical form) of a particular element at a particular point in the sample. Alternatively, one can take advantage of the fact that the excitation profile for each chemical form of an element has a slightly different energy dependence (that is, as noted above, each chemical form has a different XANES spectrum). In simple XRF imaging, samples are illuminated with high-energy X-rays so that all chemical forms are excited with equal probability. In XANES imaging, an XRF image is excited using several different X-ray energies in the XANES region. Each chemical form of an element will have a slightly different excitation probability at each wavelength. By measuring multiple maps at several different excitation energies, it is possible to tease apart the spatial distributions of each of the chemical forms of an element. Differences in the different imaging methods are illustrated schematically in Figure 2.

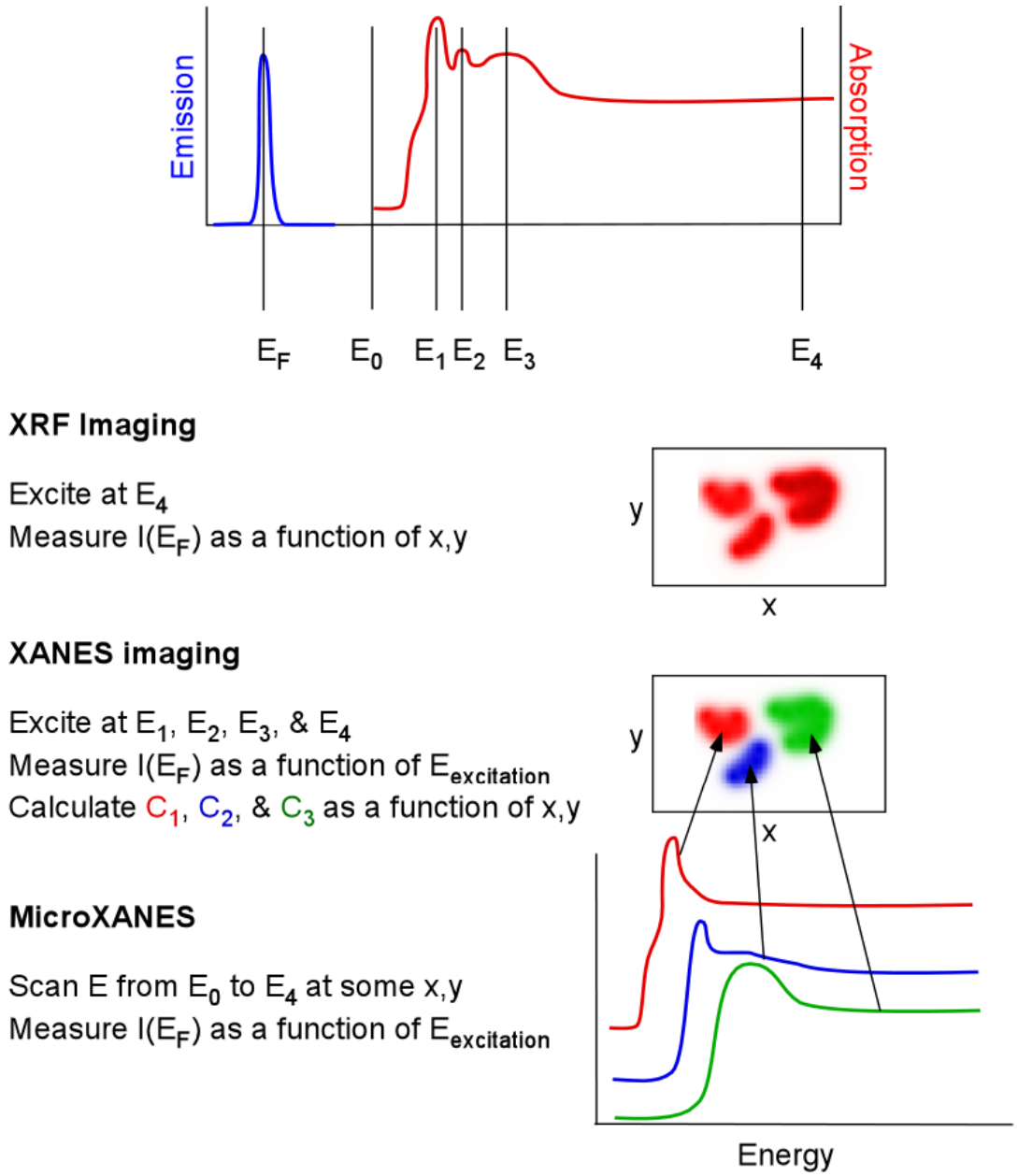

Figure 2: Schematic illustration of XRF imaging experiments for a sample that has the *average* absorption spectrum shown in red. Because all forms of the element emit with nearly the same emission, there is only a single resolved x-ray fluorescence peak, shown in blue. For XRF imaging, the sample is excited well above the edge (E_4) and the XRF intensity is measured as a function of the location (x,y) that is excited. The resulting pattern gives an elemental map with no chemical information. If the peaks at E_1, E_2, and E_3 are due to different chemical species (**1**, **2**, and **3**), it is possible to perform XANES imaging by measuring XRF at each energy and calculating the relative concentration of each: C_1, C_2, and C_3 (typically measurements at several additional energies are necessary to obtain a robust solution). In this illustration, each species is well separated spatially (middle image). Finally, by measuring a full XAS spectrum with a microbeam, it is possible to obtain spatially resolved XAS spectra. In this simplified example, spectra measured at the point marked by the three arrows are the spectra for pure **1**, **2**, and **3.**

MATERIALS

Purified Protein XAS

Samples for single molecule XAS metalloprotein studies should be homogeneous with no unbound metal, since the data being collected is the average of protein sites that utilize the excited metal. The technique is buffer and pH independent, so samples can exist under a variety of solution conditions. Samples are generally measured at low temperature as frozen solutions in order to minimize thermal disorder and, more importantly, to limit the extent of X-ray induced radiation damage. As mentioned earlier, glassing agents such as glycerol are generally added at ca. 30% by volume to ensure homogeneous sample glassing and prevent ice formation. Samples can have multiple different elements, as the technique is element specific, however the same metal at two independent sites in the metalloprotein will appear as the average. Sample cell dimensions are specific for the cryostat being used and cryostats differ at different X-ray facilities. Sample cells are generally constructed from metal free materials such as Lucite (Bencze et al., 2007). Cells can be a variety of shapes and sizes, although they generally have one long open window that is placed incident to the incoming radiation. This exposed window is usually wrapped in metal free kapton tape to prevent sample loss.

Because they are so dilute, biological XAS spectra are almost always measured as fluorescence excitation spectra. In this experiment, the characteristic X-ray fluorescence intensity is monitored as the excitation energy is scanned. In the limit of thin or dilute samples, fluorescence intensity is proportional to X-ray absorption cross-section. Most modern XAS beam lines are equipped with a solid-state energy-resolving X-ray fluorescence detector.

Whole Cell XAS

Many strategies have been utilized to prepare whole cell XAS samples. In order to achieve good signal to noise ratios, the concentration of the metal within the cell must first be considered. In some cases it may be sufficient to prepare a monolayer of confluent cells or directly use bacterial cells in a cell culture. If metal concentrations within the cells are low (sub micromolar range), one may consider harvesting a population of cells into a small volume to increase the amount of sample being exposed to the X-ray beam and hence increase the signal intensity. This has been done simply by filtration of a bacterial culture using a 0.2 μm filter, sandwiching the filter paper between layers of Kapton tape followed by flash freezing in liquid nitrogen. Others have harvested cells by centrifugation and placed the collected cells directly into a 140 μL Lucite XAS sample cell using a customized set-up.

X-ray Fluorescence Imaging

Perhaps the most important part of an imaging experiment is the focused X-ray beam. Reflective optics (e.g., Kirkpatrick-Baez mirrors (Kirkpatrick and Baez, 1948)) work well for beam sizes down to ~ 1 μm and are thus well suited for XRF imaging of mm scale sample (e.g., intact tissue samples). Better spatial resolution, down to ~100 nm or better, can be achieved with zone-plate optics (Cai et al., 2003; Schroer, 2006). Samples for XRF imaging are typically placed on an X-ray transparent substrate such as ultra thin (~100 nm) silicon nitride. The mechanical systems that are used to position the sample relative to the X-ray beam need to have precision and stability that is better than the desired spatial resolution. Fortunately, most of the synchrotron laboratories have one or more beam lines dedicated to XRF imaging, including all of the necessary focusing and sample positioning hardware, together with the standard XAS hardware for tunable X-ray excitation and energy-resolved X-ray fluorescence detection.

DISCUSSION

Examples of how these X-ray techniques have been applied in order to address specific questions regarding the cellular utilization of metals are provided in the follow section. These applications include specific examples that cover excitation of a variety of different elements including both metals and non-metals.

Purified Protein XAS

Numerous laboratories have utilized XAS to answer structural and functional questions regarding many different metalloproteins. We have chosen three specific examples, from the long library of protein XAS studies, which illustrate how the technique was used to address specific questions regarding metal(s) bound to a protein. These examples are outlined in detail below: superoxide reductase (SOR) from *Pyrococcus furiosus*, which was used to determine mechanistic issues regarding the enzyme's active site; particulate methane monooxygenase (pMMO) from *Methylococcus capsulatus,* a multimetal/multinuclear system in which each metal was characterized; and the zinc finger domain of the ubiquitin binding protein Npl4, where the Zn XAS parameters were utilized in combination with NMR structure determination of the protein. In addition to structural insight, XAS can in some cases provide insight into reaction dynamics. As an example, we discuss the time resolved XAS of the zinc site in alcohol dehydrogenase (ADH), showing structural changes during catalysis.

Although the *in vivo* function of this protein is unknown, SOR is believed to provide a mechanism to combat against oxidative stress in anaerobes, which typically lack superoxide dismutate, by reducing superoxide to hydrogen peroxide (Imlay, 2002). To elucidate the role of iron in enzymatic activity, the mononuclear Fe metal center was characterized in both the ferric and ferrous oxidation states by XAS (Clay et al., 2002). Iron in the ferric form is high spin and six coordinate, with a coordination geometry constructed by four equatorial histidyl ligands, an axial cysteinate and a monodentate glutamate ligands. Fe(III) EXAFS data were best fit using one Fe-S at 2.36 Å and five Fe-N/O bonds at an average distance of 2.12 Å. In the reduced state, the ferrous site of SOR was shown to have square-pyramidal coordination geometry with four equatorial histidines and one axial cysteine; Fe EXAFS data for this sample were best fit by one Fe-S at 2.37 Å and four Fe-N/O at an average distance of 2.15 Å. A ligand for the iron can be substituted in the oxidized form, and the vacant site can be populated in the ferrous form by cyanide, which acts as a molecular mimic for superoxide. The ability to bind exogenous ligands in both the ferrous and ferric sites of SOR was suggested to be consistent with an inner-sphere catalytic mechanism involving superoxide binding at the ferrous site to yield a ferric-(hydro)peroxo intermediate. Additional mechanistic insight was supplied by characterizing the sulfur K-edge XAS for the cysteine bound to the iron in SOR (Dey et al., 2007). XANES analysis of the sulfur edge indicated that the thiolate is a highly anionic covalent ligand; the anionic character of the thiolate most likely increases the $p\mathrm{K}_a$ of the Fe(III)-OOH intermediate, facilitating protonation and eventual release. Combined, these studies paint a structural picture of how the ligand environment facilitates catalytic turnover during enzymatic activity.

Particulate methane monooxygenase is a multicopper membrane bound enzyme that catalyzes the oxidation of methane to methanol in methantropic bacteria. Prior to complete structural characterization of this multicomponent enzyme, Cu K-edge XAS studies were utilized to determine the average oxidation state and provide structural details regarding copper bound to pMMO. Initial Cu XANES spectra of as isolated Bath pMMO indicated a near equal distribution of Cu(I) and Cu(II) for the ca. 4 coppers bound to the protein, based on general edge features and the observation of both 1s→3d and 1s→4p electronic transitions apparent in the edge(Lieberman et al., 2003). Subsequent reports confirmed the protein could be prepared in a homogeneous metal oxidation state (Lieberman et al., 2006). EXAFS analysis of the as isolated protein confirmed the presence of a dinuclear Cu center, with a copper separation of 2.51 Å, and showed that the Cu-Cu distance increases to 2.65 Å when the metal is fully reduced. The remaining ligands were completely oxygen/nitrogen based and located at an average distance of 1.97 Å and 2.22 Å in the as isolated

protein and 1.98 Å and 2.14 Å in the reduced sample. The high-resolution structural details provided by XAS helped contribute to the correct assignment of the high-resolution crystal structure of pMMO (Lieberman and Rosenzweig, 2005).

Protein ubiquitination plays an important role in a variety of cellular processes. Ubiquitinated proteins are directed into the different cellular pathways through interactions with effecter proteins that contain conserved ubiquitin binding motifs. The solution structure of one such motif, NZF, was solved utilizing the metrical parameters of the metal center provided by Zn K-edge XAS studies (Wang et al., 2003). Simulations of the Zn EXAFS showed zinc was bound to four sulfur atoms at an average bond length of 2.33 Å. The Debye-Waller factor, a measure of metal-ligand bond disorder. was 0.00454 $Å^2$ indicating the average zinc-ligand environment was most likely distorted. During the solution structural calculations, the Zn bond lengths obtained by XAS were used as constraints while the value for the Debye-Waller factor was utilized to generate limits for these distance constraints. XAS is therefore an effective tool that can be used to provide unique structural details not attainable by other techniques, especially in the case of the generally spectroscopic metals like zinc.

ADH catalyzes the oxidative conversion between alcohols and aldehydes or ketones. The catalytic active site of *T. brockii* ADH contains a zinc ion bound to a single cysteine, histidine, aspartate and a glutamate. Prior to this study, two catalytic mechanisms were proposed for the protein: the first required a 4 coordinate Zn intermediate generated from water displacement at the Zn site, the second mechanisms involved a 5 coordinate Zn site where the water, rather than being displaced acts as a site for transient proton transfer. In a very interesting application of XAS, Sagi and coworkers utilized time-resolved freeze-quench XAS to trap TbADH during multiple stages within a single catalytic turnover cycle, hence providing snapshots of the zinc site during turnover (Kleifeld et al., 2003). Two distinct intermediates were detected during the mixing time range of 3 and 70 ms, and bound Zn was pentacoordinate at each step. Intermediate 1 (IM1) detected between 3-5 ms, and IM2, detected between 15-19 ms after mixing, both had 4 O/N and 1 S ligands bound to Zn nearest; however, there was a distinct ca. 0.15 Å expansion in two Zn-O/N bond lengths relative to the starting Zn-ligand complex. Results from this study allowed the authors to select the more appropriate proposed catalytic mechanism by supplying the appropriate structural details regarding the catalytic Zn site in the enzyme.

An additional immerging application of the technique involves the detailed characterization of the near edge XANES data for metal containing systems using the multiple scattering edge simulation package MXAN. Utilized recently by the Hodgson and Hedman groups, MXAN analysis

was applied to characterize the mononuclear copper complex $[Cu(TMPA)(OH_2)](ClO_4)_2$ (Sarangi et al., 2005). When applied to this copper complex, that authors nicely illustrated the utility of the technique for accurately abstracting geometric information of the metal center from an XAS spectrum. When coupled with the highly accurate bond lengths obtained from EXAFS analysis, MXAN can be incorporated to provide an accurate metal-ligand geometric picture of homogeneous metal centers for biomolecules.

Whole Cell XAS

Numerous published reports utilized whole cell XAS to determine the overall metal speciation within different cell lines. The following section highlights three examples of how the technique was applied at the cellular level and in the process nicely illustrate the range of applications for this method towards addressing diverse biological and environmental questions. In the first report, whole cell studies were used to investigate the high concentration of vanadium in the blood of subtidal marine organisms. In the second report, whole cell XAS studies were utilized to determine metal chelation strategies for five different zinc tolerant microbes found in a highly zinc-contaminated lake. In the final report, whole cell XAS was used to quantitate the generally spectroscopically silent sulfur contained within equine blood.

Tunicates are fascinating subtidal marine organisms in that some species, such as *Ascidia nigra* and *Ascidia ceratodes,* have the ability to accumulate and concentrate vanadium to levels over a million fold higher than found in seawater. Although the reason for this unusual storage ability remains unknown, much work has been done to determine the method of uptake and storage of metal in each system. Vanadium resides in multiple cell types within the blood of these organisms and interestingly the V-containing cells and the chemical speciation of metal differ even between closely related organisms. In the report by Frank and coworkers, whole cell XAS of blood cell samples from *A. nigra* and *A. ceratodes* were used to investigate species dependent differences for V distribution, which may have possible taxonimical implications (Frank et al., 1998). Subtle differences between XANES spectra for each sample were identified, confirming a unique global V environment in each cell. A shoulder in the XANES region of intact *A. ceratodes* blood cells occurred at 5476 eV, closely matching the feature found for V(III) in *aquo-*VSO_4^+. In contrast, the large 1s→3d pre-edge transition of *A. nigra* indicated ~25% of the V in this species closely matches the vanadyl ion ($[V(IV)=O]^{2+}$), which has a characteristic feature at 5468.6 eV. The edge energies for these two species differ by approximately 1 eV (5480.5 eV for *A. ceratodes* vs. 5479.5 eV for *A. nigra* samples), suggesting the remaining V(III) found in *A. nigra* has a different ligation environment

from that in *A. ceratodes*. These differences suggest unique vanadium storage distributions between species, despite the fact that the biochemical mechanisms responsible for V uptake and storage appear to be very similar.

The rise in industrialization over the past few centuries has led to environmental contamination of areas surrounding large manufacturing facilities. Operations such as smelting introduce high levels of Zn into local water supplies. Decontamination of these areas requires an understanding of metal mobility, toxicity and reactivity beginning with an understanding of the Zn speciation in metal-contaminated areas. In one such study, Webb and coworkers identified 5 bacterial anaerobes that were able to thrive in the Zn contaminated waters of lake DePue (IL) (Webb et al., 2001). These microbes were collected and grown in a laboratory setting using high Zn media. Whole cell XAS was used to determine the peptide coordination of the metal. Fitting analysis revealed unique global Zn coordination in all five species. One isolate showed Zn ligation solely by sulfur (4 S at an average bond distance of 2.34 Å), two had mixed sulfur and oxygen/nitrogen coordination (3 S at average bond distances of 2.34 Å and 1 O/N at 1.97 Å, or 2 S at 2.34 Å and 2 O/N at 1.96 Å), while the final two showed all oxygen/nitrogen ligation (4 O/N at 1.96 or 5 O/N at 1.97Å). The data were consistent with the low-Z (i.e., "O") ligands coming from phosphoryl groups. Given the number of phosphate groups located outside the cell (i.e., at the level of the cell membrane), these results may suggest that O/N dominated microbes may bind/store Zn on their outer cell surface while the S ligand dominated microbes may store Zn within the cell.

Although not a metal, sulfur is one of the essential elements most easily studied by XAS, since there are dramatic spectral variations between different chemical forms of the element. Relatively little is known about the chemical reactivity of sulfur *in vivo* due to the limited number of direct methods that can be used to study it. Its ability to cycle between different redox states makes it useful in numerous life processes towards regulating oxidation chemistry, as well as for serving as a soft base for metals themselves. Its high abundance in the cell make it perfectly suited for XAS studies, as this technique is extremely sensitive for detecting structural and redox state changes. As a proof of concept, Pickering and coworkers were able to quantitate sulfur speciation in intact equine blood cells without chemical manipulations of the sample using K-edge XAS (Pickering et al., 1998). By fitting empirical data with linear combinations of spectra from a model library, they were able to determine the relative quantities different sulfur species within samples. The authors observed sulfur within red blood cells to be 21.4% disulfide, 54.4% thiol, 21.3% thioether, 2.1% sulfoxide and 0.8% sulfate. In contrast to the intact erythrocytes, the sulfur present in the plasma had drastically different speciation: 76.5% disulfide, 20.6% thiol, 0% thioether, 0% sulfoxide, and

2.9% sulfate. These results provide confirmation of the conventional wisdom regarding the chemical form of intra- and extracellular sulfur in blood, namely that extracellular cysteine is predominately in a disulfide bond while intracellular sulfur is much more likely to be present as the reduced cysteine.

X-ray Fluorescence Imaging

As noted above, XRF imaging is conveniently divided into macroscopic (μm scale imaging using mirrors) and microscopic (nm scale imaging using zone plates). Macroscopic studies have examined a variety of tissues. Given the available resolution, these studies generally do not provide cellular detail, but can be used to correlate metal concentrations with histologically identifiable regions of tissue. There have been several recent reviews of (e.g., (Lankosz et al., 2007; Paunesku et al., 2006b), including a careful analysis of, the relative benefits of particle beam vs. X-ray excitation (Petibois and Cestelli Guidi, 2008) and consequently only the key points will be summarized here. Much of the interest in macroscopic-scale XRF imaging derives from attempts to correlate metal levels with disease states. One of the more interesting tissues to study is brain tissue. For example, there is substantial evidence that metals are associated in some way with Alzheimer's disease. Recent work combining XRF imaging with IR microscopy succeeded in showing that Cu and Zn co-localize specifically with the β-sheet form (i.e., the "mis-folded" form) of the amyloid beta protein that is the principle component of senile plaques in Alzheimer's disease (Miller et al., 2006). A key to this study, and to all such studies, is the development of appropriate methods (IR imaging in this case) that allow the investigator to correlate the metal levels, as seen by XRF, with specific features in the tissue.

A second area that has received significant attention is cancer, where there have been numerous attempts to correlate changes in metal levels (either essential metals such as Fe, Cu, and Zn, or toxic metals such as Cd, Cr and As) with disease state. Although this work remains largely phenomenological at this point, it is clear that there exist many tantalizing differences in metal status between diseased and healthy tissue. The challenge, and also the promise, of such studies will lie in sorting out cause and effect. That is, is a low, or high, level of a particular metal a cause or a symptom of the disease?

One approach to disentangling cause and effect is to treat samples with different concentrations of the element of interest (e.g., a toxic element) and follow the distribution of this element through the sample in both space and time (Isaure et al., 2006; Mesjasz-Przybylowicz et al., 2007). Much of this sort of work has been done on plants because of their ease of manipulation.

One of the first such examples was an elegant study by Pickering et al. (Pickering et al., 2000) that used XANES imaging to study the distribution and speciation of selenium in plants that had been exposed to 5 mM selenate. By measuring the absorbance, the X-ray scatter, and the X-ray fluorescence at two different excitation energies, they were able to determine that Se is present predominantly as selenate in the mature leaf tissue while young leaves and roots contain almost exclusively organoselenium, an observation that may be helpful in understanding the biological basis of selenium hyper-accumulation in some plants.

XRF imaging can, in principle, be used for elements as light as phosphorus (or even lighter with the use of vacuum sample chambers). For heavy elements (e.g., first transition series metals and higher), X-ray absorption by the sample is relatively unimportant, at least for samples that are no more than a few hundred μm thick. However, attenuation by the sample can be quite important for thick samples, leading to apparent heterogeneities in composition (i.e., light elements appear to be depleted from the far side of the sample because the fluorescence is absorbed by the intervening sample (Mesjasz-Przybylowicz et al., 2007). A second difficulty with XRF studies of light elements is that, even if the sample is thin and dilute *on average*, the *local* concentration of the element of interest may still be large enough to significantly distort the spectrum. This is important, for example, in studies of sulfur metabolism by sulfur bacteria, where sulfur is present as globules of essential pure sulfur, which can significantly distort the resulting XANES spectrum (Pickering et al., 2001).

Most XRF imaging studies have used thin, flat sample, and have thus obtained only two-dimensional data. For three-dimensional samples, one can measure data at several different angles and use the resulting data to infer localization (Young et al., 2007), and complete three-dimensional information is available if full tomographic measurements are done. A beautiful demonstration of the ability of the latter to provide biologically relevant information was a study by Kim et al. (Kim et al., 2006) showing that iron is specifically accumulated in the provascular system of *Arabidopsis* seeds. Many studies have been carried out on chemically fixed samples, but recent work on cryogenically fixed samples suggest this may be a viable approach (Kanngiesser et al., 2007) for preparing samples that are closer to biologically-relevant wet conditions.

The discussion above focused on macroscopic XRF imaging. Increasingly, however, additional studies have focused on nm scale imaging. With this resolution, it is possible to determine directly the intracellular variations in metal concentration. Once again, there are a variety of possible biological applications (Fahrni, 2007; Paunesku et al., 2006a). A representative example is the study by Finney and co-workers of the role of copper in angiogenesis (Finney et al., 2007). It has

long been known that copper is important in angiogenesis, and there have been suggestions that by modifying Cu metabolism (e.g., with Cu specific chelators), it may be possible to inhibit angiogenesis, and thus interfere with tumor growth. X-ray nanoprobe images of individual cells showed that during angiogenesis, the bulk of the intracellular Cu is relocalized to the tips of nascent endothelial cell filopodia and across the cell membrane, providing direct evidence for the role Cu plays. Interestingly, Cu chelation, while disrupting angiogenesis, had little effect on the observed Cu relocalization. The ability to determine metal concentrations with sub-cellular resolution was critical to this work. A variety of other groups have used analogous studies to explore the effect of metals (both toxins and metallodrugs) on cells, exploring both the localization of the added compound and the effect that it has on cellular metal metabolism. Although the available X-ray resolution is ~100 nm, and even better resolution should still be possible, it can nevertheless be challenging to determine the precise localization of a particular element since the cell thickness is typically much more than 100 nm, and therefore 2-dimensional metal distributions are, in reality, the average of the spatial distribution across the cell. In practice, this means that it is often only possible to distinguish between cytoplasm and nucleus, but not to identify finer scale structures, unless one looks at thin sections cut from a cell (Dillon et al., 2002).

The lower flux and smaller sample volumes in nanoprobe studies mean it is difficult to perform full XANES imaging studies analogous to those discussed above for microprobe imaging. However, even here some spectra resolution is possible, demonstrating, for example, that most of the copper in NIH 3T3 fibroblasts is present as Cu(I) (Yang et al., 2005).

SUMMARY

As synchrotron capabilities have developed, the applications of X-ray absorption spectroscopy to biology have grown to the point that this is now a mature field. For most purified proteins, it is now (relatively) straightforward to obtain direct structural information for the metal site using XAS. This information is complementary to that available from crystallography, and is often critical to understanding the structural and chemical properties of the protein. It is possible, but more challenging, to extend these studies to more complex samples, for example heterogeneous whole-cell samples or time-dependent samples, but even these studies are becoming more common. Focused X-ray beams can also be used for elemental imaging, providing information similar to that available from particle beam microscopy, but with greater sensitivity to heavy elements, and much greater tolerance for “wet” samples. While far from routine, X-ray microprobe studies of macroscopic samples (e.g., biological tissues) and X-ray nanoprobe studies of microscopic samples (e.g., single

cells) are increasingly being used to interrogate sub-cellular distributions of elements. Much remains to be learned about the normal variability of metal concentrations within healthy cells before it will be possible to interpret the effect of drugs and disease on metal distributions. Nevertheless, it is clear that X-ray fluorescence imaging has the potential to revolutionize the study of metal ions in biology.

ACKNOWLEDGEMENTS

This work was supported in part by grants from the National Institutes of Health (DK068139 to TLS, GM38047 and GM70545 to JEPH).

REFERENCES

Ascone, I., et al., 2003. Introductory overview: X-ray absorption spectroscopy and structural genomics. Journal of Synchrotron Radiation. 10, 1-2.

Bencze, K. Z., et al., X-Ray Absorption Spectroscopy. In: R. A. Scott, C. M. Lukehart, Eds.), Applications of Physical Methods in Inorganic and Bioinorganic Chemistry: Handbook, Encyclopedia of Inorganic Chemistry, 2nd Edition. John Wiley & Sons,LTD, Chichester, UK, 2007, pp. 513-28.

Cai, L. Z., et al., 2003. Phase-shift extraction and wave-front reconstruction in phase-shifting interferometry with arbitrary phase steps. Optics Letters. 28, 1808-1810.

Clay, M. D., et al., 2002. Spectroscopic studies of Pyrococcus furiosus superoxide reductase: implications for active-site structures and the catalytic mechanism. J Am Chem Soc. 124, 788-805.

Dey, A., et al., 2007. Sulfur K-edge X-ray absorption spectroscopy and density functional theory calculations on superoxide reductase: role of the axial thiolate in reactivity. J Am Chem Soc. 129, 12418-31.

Dillon, C. T., et al., 2002. Hard X-ray microprobe studies of chromium(VI)-treated V79 Chinese hamster lung cells: intracellular mapping of the biotransformation products of a chromium carcinogen. J. Biol. Inorg. Chem. 7, 640-645.

Fahrni, C. J., 2007. Biological applications of X-ray fluorescence microscopy: exploring the subcellular topography and speciation of transition metals. Curr Opin Chem Biol. 11, 121-7.

Finney, L., et al., 2007. X-ray fluorescence microscopy reveals large-scale relocalization and extracellular translocation of cellular copper during angiogenesis. Proc Natl Acad Sci U S A. 104, 2247-52.

Frank, P., et al., 1998. Vanadium K-edge x-ray absorption spectroscopy reveals species differences within the same ascidian genera. A comparison of whole blood from Ascidia nigra and Ascidia ceratodes. J Biol Chem. 273, 24498-503.

Gnida, M., et al., 2007. Sulfur X-ray absorption spectroscopy of living mammalian cells: an enabling tool for sulfur metabolomics. In situ observation of uptake of taurine into MDCK cells. Biochemistry. 46, 14735-

41.

Imlay, J. A., 2002. What biological purpose is served by superoxide reductase? J Biol Inorg Chem. 7, 659-63.

Isaure, M. P., et al., 2006. Micro-chemical imaging of cesium distribution in Arabidopsis thaliana plant and its interaction with potassium and essential trace elements. Biochimie. 88, 1583-1590.

Kanngiesser, B., et al., 2007. Three-dimensional micro-XRF under cryogenic conditions: a pilot experiment for spatially resolved trace analysis in biological specimens. Analytical And Bioanalytical Chemistry. 389, 1171-1176.

Kim, S. A., et al., 2006. Localization of iron in Arabidopsis seed requires the vacuolar membrane transporter VIT1. Science. 314, 1295-8.

Kirkpatrick, P., Baez, A. V., 1948. Formation of Optical Images by X-Rays. J. Opt. Soc. Am. 38, 766-777.

Kleifeld, O., et al., 2003. Active site electronic structure and dynamics during metalloenzyme catalysis. Nat Struct Biol. 10, 98-103.

Lankosz, M., et al., 2007. Elemental imaging of human brain glioma tissue with the use of synchrotron radiation. Acta. Neuropathologica. 114, 317-318.

Lieberman, R. L., et al., 2006. Characterization of the Particulate Methane Monooxygenase Metal Centers in Multiple Redox States by X-ray Absorption Spectroscopy. Inorg Chem. 45, 8372-8381.

Lieberman, R. L., Rosenzweig, A. C., 2005. Crystal structure of a membrane-bound metalloenzyme that catalyses the biological oxidation of methane. Nature. 434, 177-82.

Lieberman, R. L., et al., 2003. Purified particulate methane monooxygenase from Methylococcus capsulatus (Bath) is a dimer with both mononuclear copper and a copper-containing cluster. Proc. Natl. Acad. Sci. USA. 100, 3820-5.

Mesjasz-Przybylowicz, J., et al., 2007. Comparison of cytology and distribution of nickel in roots of Ni-hyperaccumulating and non-hyperaccumulating genotypes of Senecio coronatus. Plant And Soil. 293, 61-78.

Miller, L. M., et al., 2006. Synchrotron-based infrared and X-ray imaging shows focalized accumulation of Cu and Zn co-localized with beta-amyloid deposits in Alzheimer's disease. Journal Of Structural Biology. 155, 30-37.

Paunesku, T., et al., 2006a. X-ray fluorescence microprobe imaging in biology and medicine. J Cell Biochem. 99, 1489-502.

Paunesku, T., et al., 2006b. X-ray fluorescence microprobe imaging in biology and medicine. Journal Of Cellular Biochemistry. 99, 1489-1502.

Petibois, C., Cestelli Guidi, M., 2008. Bioimaging of cells and tissues using accelerator-based sources. Anal Bioanal Chem. 391, 1599-608.

Pickering, I. J., et al., 2001. Analysis of sulfur biochemistry of sulfur bacteria using X-ray absorption spectroscopy. Biochemistry. 40, 8138-45.

Pickering, I. J., et al., 1998. Sulfur K-edge X-ray absorption spectroscopy for determining the chemical speciation of sulfur in biological systems. FEBS Lett. 441, 11-4.

Pickering, I. J., et al., 2000. Quantitative, chemically specific imaging of selenium transformation in plants. Proc Natl Acad Sci U S A. 97, 10717-22.

Sarangi, R., et al., 2005. MXAN analysis of the XANES energy region of a mononuclear copper complex: applications to bioinorganic systems. Inorg Chem. 44, 9652-9.

Schroer, C. G., 2006. Focusing hard x rays to nanometer dimensions using Fresnel zone plates. Phys. Rev. B 74, 0334051-4.

Scott, R. A., 1985. Methods in Enzymology.

Tobin, D. A., et al., 2003. Structural characterization of the zinc site in protein farnesyltransferase. J Am Chem Soc. 125, 9962-9.

Wang, B., et al., 2003. Structure and ubiquitin interactions of the conserved zinc finger domain of Npl4. J Biol Chem. 278, 20225-34.

Webb, S. M., et al., 2001. An EXAFS study of zinc coordination in microbial cells. J Synchrotron Radiat. 8, 943-5.

Yang, L., et al., 2005. Imaging of the intracellular topography of copper with a fluorescent sensor and by synchrotron x-ray fluorescence microscopy. Proc Natl Acad Sci U S A. 102, 11179-84.

Young, L., et al., 2007. Inferring the geometry of fourth-period metallic elements in Arabidopsis thaliana seeds using synchrotron-based multi-angle X-ray fluorescence mapping. Annals Of Botany. 100, 1357-1365.